

Crossing the ballistic-ohmic transition via high energy electron irradiation

Elina Zhakina,^{1,2,*} Philippa H. McGuinness^{1,2,†} Markus König,¹ Romain Grasset³, Maja D. Bachmann,^{1,2} Seunghyun Kim,¹ Carsten Putzke,^{4,5} Philip J. W. Moll,^{4,5} Marcin Konczykowski³, and Andrew P. Mackenzie^{1,2,‡}

¹Max Planck Institute for Chemical Physics of Solids, Nöthnitzer Straße 40, 01187 Dresden, Germany

²Scottish Universities Physics Alliance, School of Physics & Astronomy, University of St. Andrews, St. Andrews KY16 9SS, United Kingdom

³Laboratoire des Solides Irradiés, CEA/DRF/IRAMIS, Ecole Polytechnique, CNRS, Institut Polytechnique de Paris, F-91128 Palaiseau, France

⁴Microstructured Quantum Matter Group, MaxPlanck Institute for Chemical Physics of Solids, 01187 Dresden, Germany

⁵Institute of Materials, École Polytechnique Fédérale de Lausanne, 1015 Lausanne, Switzerland



(Received 15 November 2022; revised 7 February 2023; accepted 9 February 2023; published 10 March 2023)

The delafossite metal PtCoO₂ is among the highest-purity materials known, with low-temperature mean free path up to 5 μm in the best as-grown single crystals. It exhibits a strongly faceted, nearly hexagonal Fermi surface. This property has profound consequences for nonlocal transport within this material, such as in the classic ballistic-regime measurement of bend resistance in mesoscopic squares. Here, we report the results of experiments in which high-energy electron irradiation was used to introduce pointlike disorder into such squares, reducing the mean free path and therefore the strength of the ballistic-regime transport phenomena. We demonstrate that high-energy electron irradiation is a well-controlled technique to cross from nonlocal to local transport behavior and therefore determine the nature and extent of unconventional transport regimes. Using this technique, we confirm the origins of the directional ballistic effects observed in delafossite metals and demonstrate how the strongly faceted Fermi surface both leads to unconventional transport behavior and enhances the length scale over which such effects are important.

DOI: [10.1103/PhysRevB.107.094203](https://doi.org/10.1103/PhysRevB.107.094203)

I. INTRODUCTION

The ballistic regime, within which the electron mean free path between internal scattering events exceeds the minimum sample dimensions, can only be observed within intrinsically ultrapure materials or highly purified metallic and semiconducting crystals [1,2]. In materials with simple, highly faceted Fermi surfaces, it can become strongly directional [3,4] with an easy direction for transport. The conductivity of suitably oriented channels can be reduced below either that available in channels of any material with an isotropic Fermi surface and the same channel parameters and carrier mobility. This directional transport has potential implications for future microelectronic technologies, as well as being of fundamental interest for the study of non-local transport regimes, so it is desirable to explore its range of validity. That is the goal of this paper.

The delafossite metals PtCoO₂ and PdCoO₂ have been shown to be ideal material hosts for directional ballistics

[3–5]. Their extremely high purity (with defect levels as low as 1 in 10⁵ in the conducting Pd/Pt layers [6]), is unique among oxide metals. Due to this high purity, transport mean free paths as long as 20 μm can be observed at low temperature [7]. One of the attractive properties of the delafossite metals is their simplicity: only one highly dispersive band crosses the Fermi level, giving a single, quasi-two-dimensional Fermi surface, as demonstrated experimentally by angle-resolved photoemission and measurements of the de Haasvan Alphen effect [8–12].

Electronic transport behavior is typically determined by the momentum-relaxing scattering of the conduction electrons and is usually described semiclassically. If the momentum relaxing mean free path is much smaller than any of the other characteristic length scales of the system, as happens in an overwhelming number of materials, it is in the Ohmic regime. The relationship between current and electric field is local, even on microscopic scales, and Ohm's law holds everywhere. If, however, the mean free path becomes long enough, a nonlocal relationship can, in principle, be observed on experimentally accessible mesoscopic length scales. The majority of ballistic regime studies have concentrated on semiconductor heterostructures or monolayer graphene [13–18] rather than metals. However, recent studies of PtCoO₂ and PdCoO₂ [3,4] have shown the strongest directional ballistics observed to date.

One of the key ways to study these unconventional transport regimes is to observe the transition from nonlocal to Ohmic transport. However, in metallic systems, changing the transport regime by gating or doping, as is typical for

*elina.zhakina@cpfs.mpg.de

†philippa.mcguinness@cpfs.mpg.de

‡andy.mackenzie@cpfs.mpg.de

semiconductors, is not possible. Variation of the mean free path, and therefore the transport regime for PtCoO₂ and PdCoO₂, is achievable instead by directly changing the number of scattering centers.

Crucially for the ballistic-Ohmic crossover, these scattering centers should be pointlike defects; no large voids or columnar defects should be created, nor should foreign atoms be implanted in the crystal. High-energy electron irradiation is the ideal technique to achieve this type of disorder. The collision kinetics of 2.5 MeV electrons with much heavier atoms are close to elastic, i.e., they enable displacement of the atom from its lattice site but do not allow the displaced atom to create a significant number of additional defects. Therefore, each collision creates an individual vacancy and an interstitial atom, known as a Frenkel pair. 2.5 MeV electrons have a significant penetration depth, estimated to be ≈ 1.8 mm in delafossite metals [6]. Hence, in our typical devices, which are less than ten microns thick, the probability of any electron sustaining more than one collision is negligible [6].

A standard method to examine materials in the ballistic regime is to study electrical transport in four-terminal junctions. Within square-shaped devices, unconventional effects can occur, such as a negative nonlocal bend resistance [19,20]. In our previous work [3] we observed novel directional ballistic phenomena by varying the size of focused-ion-beam (FIB) sculpted PtCoO₂ squares with two different Fermi surface orientations: an enhanced orientation (where the Fermi surface is symmetric about the square diagonals) and a “diminished” orientation (where the Fermi surface is not symmetric about the diagonals). However, this method introduces uncertainties into the experiment, as the geometry of the sample changes between measurements. Together with the interest in directly observing the ballistic-Ohmic crossover, this drawback motivated us to perform a high energy electron irradiation experiment with ballistic-regime PtCoO₂ squares, as reported in this paper.

II. ELECTRON IRRADIATION AND DEVICE FABRICATION

Irradiation with electrons with a kinetic energy of 2.5 MeV was performed at the SIRIUS Pelletron linear accelerator operated by the Laboratoire des Solides Irradiés (LSI) at the Ecole Polytechnique in Palaiseau, France. During the irradiation, the sample was immersed in a bath of liquid hydrogen at a temperature of 22 K to ensure that the introduced defects were not mobile. As discussed above and in our previous work [6], due to the small electron mass, only pointlike Frenkel pair defects are introduced by this 2.5 MeV electron irradiation. No additional larger defects, such as columnar defects, can be created. Fourpoint *in situ* resistivity measurements were performed as described in Ref. [6].

As discussed above, PtCoO₂ has a predominately hexagonal Fermi surface [8,9,11]. In our previously reported ballistic-regime studies of delafossite square junctions, lowering/varying the symmetry of the Fermi surface orientation about the square diagonals resulted in novel phenomena not possible with a circular Fermi surface [3]. Here we retain the nomenclature introduced in Ref. [3], with two orientations of the square edges relative to the crystal axes termed enhanced

and diminished due to their different effects on the bend resistance. In the current studies, we chose to concentrate on the diminished orientation from these previous studies [see inset of Fig. 1(a)], as the behavior of an enhanced orientation square is similar to that of a material with a circular Fermi surface. In total, we fabricated three diminished orientation PtCoO₂ squares; two squares, I1 and I2, with 15 μm side; and one square, I3, with a 10 μm side length. All squares had a contact width around 5 μm . Our previous results, reported in Ref. [3], suggested that all three squares would show ballistic behavior.

We sculpted the square devices from PtCoO₂ crystals grown via methods discussed in [11,21]. The standard sample mounting method for FIB sculpting requires using a layer of epoxy to attach the crystal to a substrate, as carried out in previous transport studies of delafossite metals [5,22]. However, the high energy electron beam degrades glue quickly, motivating us to use an “epoxy-free” mounting method similar to the method in Ref [6]. A PtCoO₂ crystal, held on a ~ 25 μm thick mica substrate by electrostatic forces, was covered by a 150 nm thick sputtered gold layer. Pt contacts were then deposited in the FIB using focused ion beam induced deposition, ensuring a mechanical connection between the crystal and the substrate. To achieve a better contact resistance, a second layer of gold was sputtered over the sample, the Pt contacts, and the substrate. Crystals mounted in this way were then FIB structured into square junctions using the standard techniques described in detail in [23,24].

III. BEND VOLTAGE BEFORE IRRADIATION

To determine the strength of the ballistic behavior in the squares and inspired by the Montgomery [25] and van der Pauw [26] methods used to measure resistivity anisotropy in the Ohmic regime, we performed bend voltage measurements with two different contact configurations, as shown in the inset of Fig. 1. Bend voltage measurements in the squares can be labeled by $V_{i,j,kl}$, where the current flows between two adjacent contacts, i and j , and the voltage difference $V = V_k - V_l$ is measured across the other contacts. Thus, in the bend 1 measurement ($V_{B1} = V_{12,43}$), the current contacts and the voltage contacts are linked by a horizontal translation, whereas for the bend 2 configuration ($V_{B2} = V_{23,14}$), they are linked vertically. A simple initial measurement of the square I3, Fig. 1, compares the temperature dependence of the two bend voltages, Fig. 1(a), and the magnetoresistance of these voltages at low temperature, Fig. 1(b).

In the Ohmic regime, where the mean free path is much smaller than the device size, the triangular lattice symmetry of the conductive layer in delafossite metals ensures an isotropic in-plane resistivity. Therefore, the two bend voltages are identical [see data above 50 K in Fig. 1(a)] and follow the van der Pauw equation:

$$V_{B1,B2} = \frac{\ln 2 \rho I}{t\pi}, \quad (1)$$

where I is the applied current, t is the thickness of the device, and ρ is the resistivity of the material. According to this equation, the bend voltages are always equal, positive, and do not depend on the square side length. Across three PtCoO₂ squares, the resistivity measured at 300 K by this van der

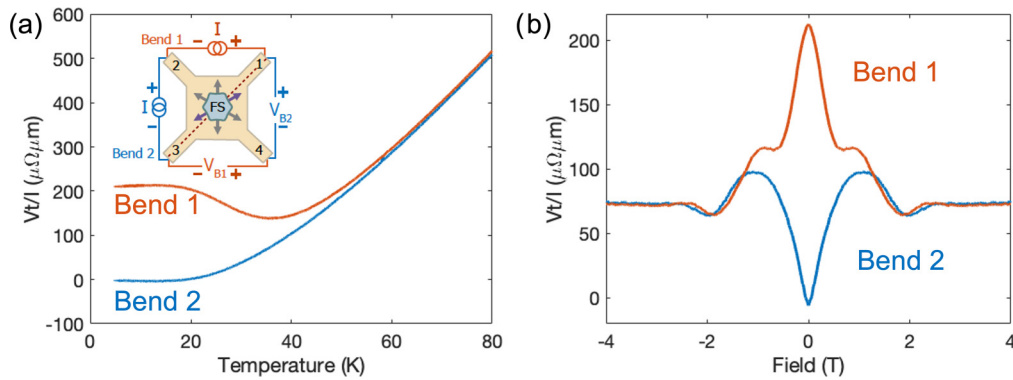


FIG. 1. (a) Temperature dependence of the bend resistance of the square I3 before irradiation below 80 K with (inset) a diagram of the contact configurations used to measure the bend voltages, bend 1 (V_{B1}) and bend 2 (V_{B2}), shown on a diminished orientation square. (b) Magnetic field dependence of the bend resistance at 5 K before irradiation.

Pauw technique before irradiation was ρ (300 K) = $1.8 \text{ \AA} \pm 0.1 \text{ } \mu\Omega\text{cm}$, in good agreement with the accepted value of $1.82 \text{ } \mu\Omega\text{cm}$ [7]. However, Eq. (1) is not valid within the ballistic regime due to its highly nonlocal nature. Indeed, in this regime, when the majority of the injected electrons pass along the square diagonal to the negative voltage contact, the bend voltages $V_{B1,B2}$ become negative. These voltages also need not be equal: our previous study with PtCoO₂ and PdCoO₂ [3] reported the first dependence of the bend voltage on the orientation of the contacts within a material with isotropic conductivity in the Ohmic regime, made possible due to the lower symmetry of their Fermi surfaces. Since we are no longer measuring the resistivity in the traditional sense, we label the y axes in Fig. 1 as Vt/I rather than ρ , although the two quantities have the same units, and we refer to both as resistivity when describing them narratively. All square devices have different intrinsic thicknesses from crystal growth; therefore, unit Vt/I includes the thickness, t , to automatically account for these differences and allow for numerical comparison between squares.

As expected within the Ohmic regime, at temperatures above 70 K, there is little dependence of the voltage on the contact configuration. As shown in Fig. 1(a), at low temperatures, where the diagonal transport is reduced, the bend 2 voltage becomes negative, showing similar behavior to materials with circular Fermi surfaces deep within the nonlocal ballistic regime. However, the bend 1 data increase as the temperature is reduced, and show peak at zero field at low temperatures [Fig. 1(b)], signifying a strong transport anisotropy present only within the ballistic regime. This anisotropy between the two bend measurements cannot be observed in materials with circular Fermi surfaces or with a Fermi surface orientation which is symmetric about the square diagonals. The advantageous combination of an extremely long mean free path and a hexagonal Fermi surface in delafossite metals opens a nonlocal transport regime. Our goal here is to study the limits of that regime at low temperatures.

IV. *IN SITU* MEASUREMENTS

The critical parameter that determines the strength of the ballistic behavior in our squares is w/l , where l is the mean free path of the device and w is the width of the square.

Although the Ohmic-ballistic crossover can in principle be examined by varying w , as carried out in our previous work [3] where the square width was gradually reduced using a FIB, the inevitable uncertainties in geometry between thinning down steps can cause significant inaccuracy in measurements, particularly at smaller square sizes, and there is always a question of whether to simultaneously scale down the width of the contacts to the squares [27]. Our goal in this work was to use high energy electron irradiation to obtain a direct measurement of the effect of extra elastic scattering and a reduced mean free path on the ballistic phenomena and hence, observe the ballistic-Ohmic changeover. Using this method, the geometrical factors are determined during the initial microsculpting of the sample and do not change during the experiment.

The SIRIUS Pelletron linear accelerator allows us to perform four-point *in situ* resistance measurements and therefore monitor changes to the resistivity as a function of electron dose. However, only one voltage pair can be measured during irradiation. As the bend 1 voltage shows unusual ballistic-regime behavior most distinct from that in the Ohmic regime, we chose this pair for the *in situ* measurements.

V. *EX SITU* MEASUREMENTS

For many of the experiments that we wished to perform, *in situ* measurement was not sufficient, either because we wished to study magnetoresistance (requiring a different cryostat) or because we needed to perform a sequential cycle of *ex situ* study followed by further irradiation in order to reach high levels of disorder. Any *ex situ* measurement requires warming the devices up to room temperature, which leads to the annealing out of approximately 30% of the defects created by the low-temperature irradiation. Having measured this previously, we were able to take it into account when comparing *ex situ* measurements as a function of dose with others done *in situ*. For most of our *ex situ* data, however, we parametrize the effect of the irradiation in terms of the mean free path during the *ex situ* measurement, which automatically takes the annealing into account.

VI. DOSE DEPENDENCE OF THE RESISTIVITY

In Fig. 2, we compare, as a function of electron dose, the change in the resistivity of a larger PtCoO₂ sample, S1, which

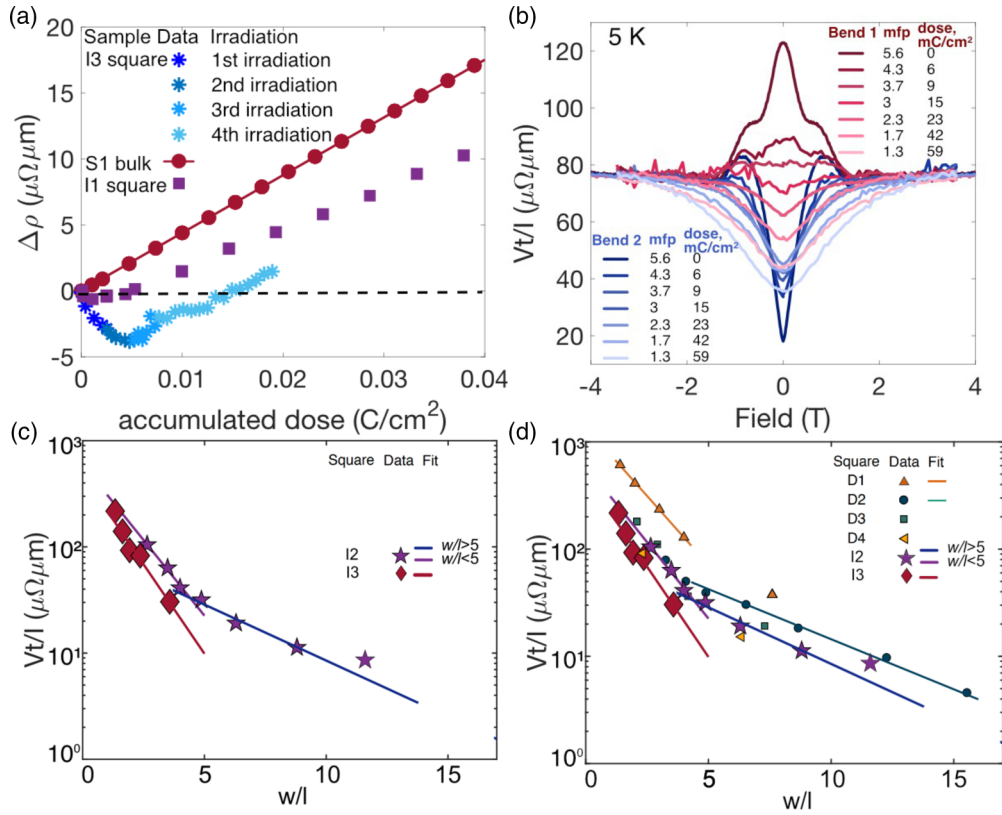


FIG. 2. (a) Resistivity increment of three PtCoO₂ samples: the bulk sample S1 and the bend 1 measurement for two diminished squares, I1 and I3. For the square I3, the data is normalized due to annealing between irradiation periods. (b) Magnetoresistance at 5 K for the diminished square I2 (with side length 15 μm) at several irradiation doses (values do not include annealing correction), normalized by the initial value at high magnetic fields. (c and d) The decay of $\Delta Vt/I$, where $\Delta V = V_{B1} - V_{B2}$ at zero field, as a function of the ratio of square side length w to the mean free path l (c) for the two diminished irradiated squares I2 and I3 and (d) including four nonirradiated diminished squares D1 to D4 [3].

is in the Ohmic regime and the bend 1 measurement of two diminished-orientation squares (I1 and I3). The dependence of the resistivity on dose for the S1 sample is linear. Our detailed defect studies of bulk PtCoO₂ in Ref. [6] prove that this resistivity increase during irradiation is dominated by the defects in the conductive Pt planes, as expected in such a strongly quasi-two-dimensional system. However, the *in situ* measurement on the larger diminished square, I1, is surprising. Before irradiation, it is in the ballistic regime, and in contrast to the behavior of the large sample, its resistivity decreases slightly on initial irradiation. To investigate this further, we performed a series of *ex situ* measurements on a smaller square, I3, correcting for the around 30% of annealed defects mentioned above. I3 is deeper in the ballistic regime than I1, and the decrease in resistivity upon dose is larger.

Even though these results seem at first glance counterintuitive, they prove the above assumption that the induced anisotropy in the ballistic regime is a result of the nonlocal transport combined with the symmetry lowering by the sample shape and the symmetry of the Fermi surface. The introduced pointlike defects decrease the mean free path of the electrons, and therefore, we observe the ballistic-Ohmic crossover. The initial drop in resistivity at small dose occurs because the bend 1 resistance was enhanced over the Ohmic-regime value by ballistic effects which are suppressed by irradiation. As the defect concentration increases, the

resistivity begins to increase for both squares, and at higher electron doses, the behavior becomes linear with a slope close to that of the bulk sample, suggesting the transport is becoming more Ohmic. Thus, the anisotropy should be suppressed, with the characteristic peak and trough in the bend 1 and bend 2 voltages in the magnetoresistance shown in Fig. 1(b) moving closer during irradiation. The fact that the effect is more pronounced in the smaller square further confirms its ballistic origin.

VII. DECAY OF ANISOTROPY IN THE MAGNETORESISTANCE

To examine the suppression of the ballistic anisotropy more quantitatively, we performed *ex situ* measurements of magnetoresistance of both bend resistances simultaneously, on squares I2 and I3. After electron irradiation, the sample was warmed to room temperature and then cooled down to 5 K *ex situ* for magneto transport measurements. In order to consider only the ballistic contribution, the additional ohmic resistance acquired during irradiation was subtracted from both sets of bend measurements. This subtraction also takes annealing after *in situ* measurements into account. The next steps of irradiation were performed in the same way. Our previous studies of bulk PtCoO₂ [6] showed that further thermal cycles of the irradiated samples do not cause the defects' annealing.

Thus, after the magnetoresistance measurements, we continued electron irradiation of the sample, considering that the defects' annealing happened only once in each of the measurement steps (after the first warmup to room temperature). To observe the smooth ballistic-Ohmic transition, we required several steps of the *ex situ* magnetoresistance measurements between electron irradiation runs; the experiment required a total of six months.

The *ex situ* magnetoresistance data from square I2 at 5 K are shown in Fig. 2(b). In the unirradiated square, the bend resistivities exhibit strong ballistic behavior dramatically different from the bulk magnetoresistance [6,22]. The bend 1 measurement peaks at zero magnetic field, and the bend 2 resistance has a trough. For the bend 2 resistance measurement, the trough becomes smaller as the dose increases. The bend 1 resistance peak at zero field also weakens dramatically with increasing dose, and, at sufficiently higher doses, becomes closer to a bulk magnetoresistance trough. However, there is still a significant difference between the two bend measurements. At high doses of electron irradiation, the trough in both measurements broadens in the magnetic field and has a magnetoresistance closer to that of a bulk, Ohmic-regime sample. This broadening of the magnetoresistance with irradiation at higher irradiation doses is similar to that observed and understood as an Ohmic-regime effect in our previous work with bulk samples [6], further suggesting that the heavily-irradiated squares are close to the Ohmic regime. At the final dose of electron irradiation without annealing correction of 0.06 C/cm^2 which equates to a Frenkel pair concentration around 0.02% [6], the two bend voltages still differ, even though they have a qualitatively similar magnetoresistance. Therefore, the I1 square was irradiated to a significantly higher dose of 1.2 C/cm^2 , resulting in the two bend voltages becoming equal and indicating a complete suppression of the ballistic anisotropy (see Appendix A below). At large field values, above around $B \approx 3 \text{ T}$, the behavior of both bend voltages becomes nearly identical, independent of irradiation dose. This suggests that electrons have tiny cyclotron orbits compared to the device size and transport becomes Ohmic.

The limits of the ballistic behavior can be still better characterized by quantifying how the anisotropy decays as a function of w/l . Estimating l in the squares has some subtleties because it should be the value that would exist in a large sample of the same purity, but careful cross-checks between several methods (see Appendix B) give consistent and, we believe, trustworthy values. The zero-field difference at 5 K between the bend voltages $\Delta Vt/I = V_{B1}(B=0) - V_{B2}(B=0)]/I$ is an ideal parameter to characterize the strength of the ballistic regime in our square devices as it is equal to zero in the Ohmic regime, ensuring the automatic subtraction of any Ohmic background. Figure 2 shows the variation of $\Delta Vt/I$ with the ratio, w/l for the two irradiated squares I2 and I3. The decay rate is similar between these two squares. However, there are two distinct regimes. At small values of w/l , the decay is more rapid. When $w/l \approx 5$, the decay becomes slower. The decay exhibits a slower rate to at least $w/l \approx 13$, far beyond the traditional limits of the ballistic regime of $w/l \approx 1$. There is also a good agreement between the data from the irradiated squares and an exponential decay with two fitted constants: $\Delta Vt/I \approx e^{-bw/l}$, providing b has two

different constant values, b_S and b_F , in the two distinct decay regimes $w/l < 5$ and $w/l > 5$.

Figure 2(d) is a comparison of the ballistic decay between the irradiated squares and our previous studies [3]. The parameter $\Delta Vt/I$ for squares D1 to D4 is defined in the same way as in Fig. 2(c) and the orientation of the Fermi surface within these squares is the same as that of the I2 and I3 squares. The only difference between the D squares and two I squares is the method used to vary the ratio w/l . In the D squares, the mean free path was constant, and we changed the width w of the squares in stages using a FIB. Despite the vastly different experimental methods, the ballistic decay is similar between the D squares and the irradiated I squares. In particular, at the value of $w/l \approx 5$, the decay changes rate in both square types.

The slopes of the decay in the two distinct regimes are also comparable, and independent of the method used to change w/l . For the rapid decay, when $w/l < 5$, the fitting constants b_F for irradiated squares I2 and I3 are $0.65 \text{ \AA} \pm 0.06$ and $0.70 \text{ \AA} \pm 0.06$ respectively, which is in good agreement with the result from the nonirradiated D squares [3]. At $w/l > 5$, the decay is a factor of three slower, with $b_S = 0.23 \text{ \AA} \pm 0.02$ for the irradiated I2 square and $b_S = 0.21 \text{ \AA} \pm 0.02$ for the D2 square. It is important to note that, in previous studies on other materials, the characteristic decay length, l/b , was always smaller than the mean free path l . However, in PtCoO₂, this length is around $1.5l$ for the rapid decay and $4.8l$ for the slow decay. As discussed in [3] the transfer junction studies reported before have been performed on materials with circular Fermi surfaces. If an electron with a circular Fermi surface is scattered by a defect in the bulk of the device, there is a vanishing chance that the direction of motion stays the same. However, there are only six primary electron directions on a hexagonal Fermi surface. Thus, the chance of the direction of motion not changing significantly after scattering increases. The observed behavior highlights the importance of carefully considering the Fermi surface symmetry when studying transport within ultrapure materials.

A further surprising aspect of these results is that the ballistic effects are not eliminated even after reaching a defect concentration of 0.02%, where the PtCoO₂ mean free path is more than a factor of 10 shorter than the square side. This is partly due to the sensitivity of having a different measurement to pick out the ballistic signature. However, a possible origin of such long-lasting ballistic effects is the presence of small-angle scattering. This scattering contributes little to the resistivity but affects electron trajectories and, therefore, strongly constrains the range of the ballistic regime in metals with circular Fermi surfaces. In PtCoO₂, however, small-angle scattering has a far smaller effect on the zero-field trajectory as, after scattering, the electron will typically be in a state on the same facet of the hexagonal Fermi surface. This suggests that small angle scattering is likely less effective in suppressing ballistic effects in PtCoO₂ than in materials with circular Fermi surfaces. The faceted Fermi surfaces of the delafossite metals therefore not only lead to previously unobserved nonlocal transport effects, but also allow them to be observed even when the mean free path falls considerably below the characteristic device size.

In conclusion, by direct variation of the mean free path via high energy electron irradiation, we have confirmed the

origins of the novel ballistic effects first observed in delafossite metals. We have introduced high energy electron irradiation as a well-controlled technique to cross from nonlocal to local transport behavior in metals and therefore determine the nature and extent of unconventional nonlocal transport behavior. This technique is general and applicable not only to delafossite metals, but a wide range of other highlyconductive materials. The results of our experiment have shown how the strongly faceted Fermi surface leads both to unconventional transport responses and to an enhanced range of parameters over which nonlocal effects are important, a finding which is expected to apply to other ultrapure materials with faceted Fermi surfaces, including those used in technological applications. In that sense we believe that our findings open novel regimes in mesoscopic physics.

ACKNOWLEDGMENTS

We thank Olivier Cavani for operating the SIRIUS accelerator. We are pleased to acknowledge useful discussions with L.W. Molenkamp and B. Schmidt. We acknowledge financial support from the Max Planck Society. P.H.M. and M.D.B. received PhD studentship support from the UK Engineering and Physical Science Research Council via Grant No. EP/L015110/1. C.P. and P.J.W.M. are supported by the European Research Council under the European Union's Horizon 2020 research and innovation programme (Microstructured Topological Materials Grant No. 715730). E. Z. acknowledges support from the International Max Planck Research School for Chemistry and Physics of Quantum Materials (IMPRS-CPQM). Irradiation experiments performed on the SIRIUS platform were supported by the French National Network of Accelerators for Irradiation and Analysis of Molecules and Materials (EMIR&A) under Project No. EMIR 2019 18-7099.

E.Z. and P.H.M. contributed equally to this work.

APPENDIX A: HIGH-DOSE IRRADIATION OF SQUARE II

During this irradiation experiment, the mean free path of the square I3 was decreased almost by a factor of four. However, this dose did not eliminate the ballistic anisotropy completely. Thus, square I1 was irradiated to a total dose of approximately 1.2 C/cm^2 . This took around twelve hours of high energy electron irradiation, and the dose is almost twenty times higher than the total irradiation dose of square I3.

Before irradiation, the magnetoresistance shown in Fig. 3, exhibited strong ballistic behavior, similar to all of the diminished-orientation squares. However, both the bend measurements are identical after irradiation, indicating that the higher dose of irradiation has completely eliminated the anisotropic ballistic effect. This reaffirms that the observed anisotropy originates a combination of the extreme mean free path and the lowered symmetry due to the device's geometry and the symmetry of the Fermi surface.

APPENDIX B: ESTIMATE OF THE MEAN FREE PATH OF IRRADIATED SQUARES

To compare the geometric and electronic transport length scales during irradiation and also between nonirradiated

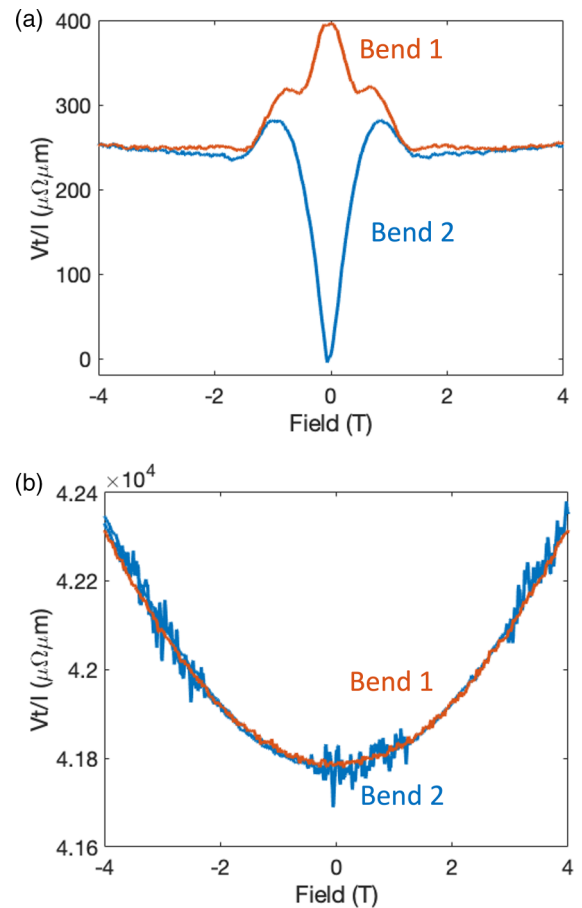


FIG. 3. Magnetoresistance at 5 K (a) before and (b) after a high dose of irradiation (1.2 C/cm^2) for the II diminished square.

squares from our previous work [3], it is crucial to accurately determine the mean free path within each irradiation step. The derivation of the mean free path from the Drude formula

$$l = \frac{m_* v_F}{n e^2 \rho}, \quad (\text{B1})$$

where m_* is the effective mass of the transport electrons, v_F is the Fermi velocity, e is the electronic charge, and n is the density of carriers, relies upon the existence of a local relationship between the current density and the electric field. However, this relationship does not exist in the ballistic regime, therefore, estimating the mean free path in the square devices during irradiation is quite challenging as the formula (B1) is invalid, and the mean free path cannot be calculated directly.

The effective mass, Fermi velocity, and density of the transport electrons are well known in PtCoO_2 [7–12]. The mean free path in an irradiated square device should be calculated for an equivalent bulk sample (with Ohmic transport behavior) with the same intrinsic purity and irradiation dose. The resistivity of such a bulk sample also increases during irradiation from ρ_0 by an additive $\Delta\rho$, which is directly proportional to the total electron dose [6].

Suppose, at high magnetic field, the transport behavior is assumed to be Ohmic. In that case, the high-field resistance

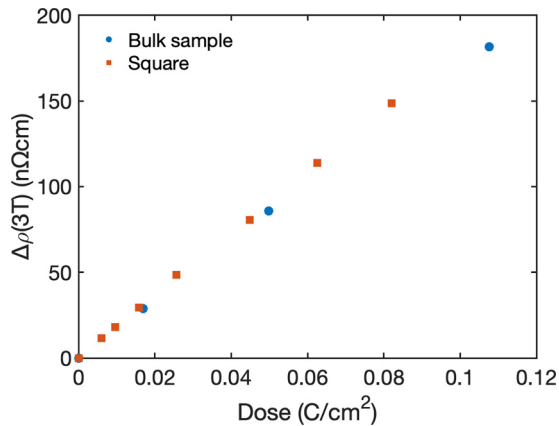


FIG. 4. Resistivity increment at 3 T for the bulk PtCoO₂ sample and ballistic square as the function of irradiation dose after annealing.

and bulk sample magnetoresistance can be used to estimate the Ohmic contribution to the resistivity of a square at zero field. This assumption is supported by the fact that the cyclotron radius above 4 T is below 1.3 μm , much less than half of the irradiation square contacts' width, thus suggesting that the electrons are less able to sense the confined experimental geometry. Figure 4 compares the resistivity increment at 3 T between the bulk PtCoO₂ sample and ballistic square device as a function of irradiation dose. The similarity of the slopes proves that the transport behavior at high magnetic field is Ohmic.

If the high-field behavior is Ohmic, the zero-field resistivity calculated in reverse from the high field resistivity of the square (using the bulk magnetoresistance values) would be the zero-field resistivity for a bulk sample of the same intrinsic

TABLE I. The calculated mean free paths of the samples I2 and I3 at each intermediate irradiation step.

Total dose, C/cm ²	I2		I3	
	l (μm)	w/l	C/cm ²	l (μm) w/l
0	5.60.1	2.680.09	0	7.40.2 1.350.03
0.006	4.30.2	3.490.15	0.003	6.00.3 1.600.03
0.009	3.70.3	4.050.20	0.007	5.10.3 1.960.09
0.015	3.00.2	5.00.2	0.010	4.20.2 2.40.1
0.023	2.30.3	6.50.5	0.0235	2.70.2 3.70.2
0.042	1.70.2	8.80.8		
0.059	1.30.2	11.51.2		

purity but where ballistic effects are negligible. The Ohmic-regime expression (B1) can then be used with this value to determine the mean free path. However, the value of the magnetoresistance also changes during irradiation. Thus, we used previous high energy irradiation studies of bulk PtCoO₂ [6] to calculate the bulk equivalent of the magnetoresistance under irradiation.

The described approach using high-field data is proven to be valid in [27] by direct comparison with application of the Ohmic formula (B1) at zero field for large 95 μm PtCoO₂ squares, yielding accurate estimates of the mean free path. This method also automatically takes the annealing between irradiation periods into account, as the mean free path is calculated from *ex situ* resistivity data at high magnetic field post this annealing. The calculated mean free paths of the samples I2 and I3 at each intermediate irradiation step, as estimated by this method, are shown in Table I.

- [1] L. Pfeiffer, K. W. West, H. L. Stormer, and K. W. Baldwin, Electron mobilities exceeding $10^7 \text{cm}^2/\text{Vs}$ in modulation-doped GaAs, *Appl. Phys. Lett.* **55**, 1888 (1989).
- [2] J. Baringhaus, M. Ruan, F. Edler, A. Tejada, M. Sicot, A. Taleb-Ibrahimi, A.-P. Li, Z. Jiang, E. H. Conrad, C. Berger *et al.*, Exceptional ballistic transport in epitaxial graphene nanoribbons, *Nature (London)* **506**, 349 (2014).
- [3] P. H. McGuinness, E. Zhakina, M. König, M. D. Bachmann, C. Putzke, P. J. W. Moll, S. Khim, and A. P. Mackenzie, Low-symmetry nonlocal transport in microstructured squares of delafossite metals, *Proc. Natl. Acad. Sci. USA* **118**, e2113185118 (2021).
- [4] M. D. Bachmann, A. L. Sharpe, G. Baker, A. W. Barnard, C. Putzke, T. Scaffidi, N. Nandi, P. H. McGuinness, E. Zhakina, M. Moravec *et al.*, Directional ballistic transport in the two-dimensional metal PdCoO₂, *Nat. Phys.* **18**, 819 (2022).
- [5] P. J. W. Moll, P. Kushwaha, N. Nandi, B. Schmidt, and A. P. Mackenzie, Evidence for hydrodynamic electron flow in PdCoO₂, *Science* **351**, 1061 (2016).
- [6] V. Sunko, P. H. McGuinness, C. S. Chang, E. Zhakina, S. Khim, C. E. Dreyer, M. Konczykowski, H. Borrmann, P. J. W. Moll, M. König *et al.*, Controlled Introduction of Defects to Delafossite Metals by Electron Irradiation, *Phys. Rev. X* **10**, 021018 (2020).
- [7] A. P. Mackenzie, The properties of ultrapure delafossite metals, *Rep. Prog. Phys.* **80**, 032501 (2017).
- [8] F. Arnold, M. Naumann, H. Rosner, N. Kikugawa, D. Graf, L. Balicas, T. Terashima, S. Uji, H. Takatsu, S. Khim *et al.*, Fermi surface of PtCoO₂ from quantum oscillations and electronic structure calculations, *Phys. Rev. B* **101**, 195101 (2020).
- [9] H. J. Noh, J. Jeong, J. Jeong, E.-J. Cho, S. B. Kim, K. Kim, B. I. Min, and H.-D. Kim, Anisotropic Electric Conductivity of Delafossite PdCoO₂ Studied by Angle-Resolved Photoemission Spectroscopy, *Phys. Rev. Lett.* **102**, 256404 (2009).
- [10] C. W. Hicks, A. S. Gibbs, A. P. Mackenzie, H. Takatsu, Y. Maeno, and E. A. Yelland, Quantum Oscillations and High Carrier Mobility in the Delafossite PdCoO₂, *Phys. Rev. Lett.* **109**, 116401 (2012).
- [11] P. Kushwaha, V. Sunko, P. J. W. Moll, L. Bawden, J. M. Riley, N. Nandi, H. Rosner, M. P. Schmidt, F. Arnold, E. Hassinger, T. K. Kim, M. Hoesch, A. P. Mackenzie, and P. D. C. King, Nearly free electrons in a 5D delafossite oxide metal, *Sci. Adv.* **1**, e1500692 (2015).
- [12] V. Sunko, H. Rosner, P. Kushwaha, S. Khim, F. Mazzola, L. Bawden, O. J. Clark, J. M. Riley, D. Kasinathan, M. W. Haverkort *et al.*, Maximal rashba-like spin splitting via

- kinetic-energy-coupled inversion-symmetry breaking, *Nature (London)* **549**, 492 (2017).
- [13] A. M. Gilbertson, M. Fearn, A. Kormányos, D. E. Read, C. J. Lambert, M. T. Emeny, T. Ashley, S. A. Solin, and L. F. Cohen, Ballistic transport and boundary scattering in InSb/InAl_{1-x}Sb mesoscopic devices, *Phys. Rev. B* **83**, 075304 (2011).
- [14] E. Matioli and T. Palacios, Room-temperature ballistic transport in III-nitride heterostructures, *Nano Lett.* **15**, 1070 (2015).
- [15] N. Goel, J. Graham, J. C. Keay, K. Suzuki, S. Miyashita, M. B. Santos, and Y. Hirayama, Ballistic transport in InSb mesoscopic structures, *Phys. E* **26**, 455 (2005).
- [16] L. Banszerus, M. Schmitz, S. Engels, M. Goldsche, K. Watanabe, T. Taniguchi, B. Beschoten, and C. Stampfer, Ballistic transport exceeding 28 μm in CVD grown graphene, *Nano Lett.* **16**, 1387 (2016).
- [17] A. S. Mayorov, R. V. Gorbachev, S. V. Morozov, L. Britnell, R. Jalil, L. A. Ponomarenko, P. Blake, K. S. Novoselov, K. Watanabe, T. Taniguchi *et al.*, Micrometer-scale ballistic transport in encapsulated graphene at room temperature, *Nano Lett.* **11**, 2396 (2011).
- [18] S. Weingart, C. Bock, U. Kunze, F. Speck, T. Seyller, and L. Ley, Low-temperature ballistic transport in nanoscale epitaxial graphene cross junctions, *Appl. Phys. Lett.* **95**, 262101 (2009).
- [19] Y. Hirayama, S. Tarucha, T. Saku, and Y. Horikoshi, Hall effect in macroscopic ballistic four-terminal square structures, *Phys. Rev. B* **44**, 3440 (1991).
- [20] G. Timp, H. U. Baranger, P. deVegvar, J. E. Cunningham, R. E. Howard, R. Behringer, and P. M. Mankiewich, Propagation around a Bend in a Multichannel Electron Waveguide, *Phys. Rev. Lett.* **60**, 2081 (1988).
- [21] P. Kushwaha, H. Borrmann, S. Khim, H. Rosner, P. J. W. Moll, D. A. Sokolov, V. Sunko, Y. Grin, and A. P. Mackenzie, Single crystal growth, structure, and electronic properties of metallic delafossite PdRhO₂, *Cryst. Growth Des.* **17**, 4144 (2017).
- [22] N. Nandi, T. Scaffidi, P. Kushwaha, S. Khim, M. E. Barber, V. Sunko, F. Mazzola, P. D. C. King, H. Rosner, P. J. W. Moll *et al.*, Unconventional magneto-transport in ultrapure PdCoO₂ and PtCoO₂, *npj Quantum Mater.* **3**, 66 (2018).
- [23] P. J. W. Moll, Focused ion beam microstructuring of quantum matter, *Annu. Rev. Condens. Matter Phys.* **9**, 147 (2018).
- [24] E. Zhakina, Investigation of transport regimes in restricted geometries of ultra-pure natural heterostructures, PhD Thesis, University of St. Andrews, St. Andrews, United Kingdom (2022).
- [25] H. C. Montgomery, Method for measuring electrical resistivity of anisotropic materials, *J. Appl. Phys.* **42**, 2971 (1971).
- [26] L. J. van der Pauw, A method of measuring the resistivity and hall coefficient on lamellae of arbitrary shape, *Philips Tech. Rev.* **20**, 220 (1958).
- [27] P. H. McGuinness, Probing unconventional transport regimes in delafossite metals, Ph.D. thesis, University of St. Andrews, St. Andrews, United Kingdom (2021).